Asian Journal of Chemistry Vol. 22, No. 6 (2010), 4617-4624

Synthesis of Ordered Bimodal Mesoporous Silica Nanoparticles from as Synthesized MCM-48

DONG TIAN* and XING ZHAO
Department of Chemistry, Huainan Normal College, Huainan-232001, P.R. China
Fax: (86)(554)6672651; Tel: (86)(554)6672637; E-mail: tiandong@mail.ustc.edu.cn

The convenient preparation of ordered bimodal mesoporous silica nanoparticles has been achieved by mild-temperature post-synthesis hydrothermal treatment of as-synthesized MCM-48 mesoporous materials in H_2O_2 solution. X-ray diffraction, TEM, FT-IR, TGA and nitrogen sorption were used to characterize the obtained bimodal mesoporous silica sample. The bimodal mesoporous MCM-48 can be obtained only under H_2O_2 hydrothermal treatment. Hydrogen peroxide plays an important role in simultaneously removing organic templates and forming ordered bimodal mesopores.

Key Words: MCM-48, Bimodal mesoporous silica, Nanoparticles, Hydrothermal treatment, H_2O_2.

INTRODUCTION

Since the discovery of M41S family in 1992[1], drastic progress in the synthesis of ordered mesoporous silica materials has been obtained due to their potential application in sorption, catalysis and separation, *etc.*[2]. Especially, there is a great deal of interest in the synthesis of mesoporous silica materials with various framework structures, pore sizes and morphologies[1,3]. Recent studies in this field are interestingly focused on the synthesis of hierarchical porous silica materials[4-11] as well as silica fine particles on a nanometer scale[12-14]. The occurrence of pores with a bimodal pore size distribution in mesoporous materials is important and useful for catalysis and for engineering of pore systems[15], because the large and small pores play a cooperative role as gas or fluid paths and molecular adsorption sites or reservoirs, leading to highly functional catalyst supports and adsorbents. Up to now, most of the hierarchical porous materials are mainly synthesized by using mixing templates method. However, such mixing templates strategy does not necessarily results in the desired bimodal mesopores, because often the co-template just leads to a unimodal pore system. Although the post-synthesis hydrothermal restructuring is a convenient synthesis route to expand the pore size of mesoporous silicas[16], there is little literature concerning the formation of bimodal mesoporous silica materials by post-synthesis hydrothermal treatment[6].

Herein, we report the first synthesis of bimodal mesoporous silica nanoparticles with a cubic mesostructure using the H_2O_2 post-hydrothermal treatment when simultaneously removing the organic templates. To the best of our knowledge, there

are no literatures which describe the hydrogen peroxide post-synthesis hydrothermal treatment can simultaneously remove templates and form ordered bimodal mesoporous silica materials.

EXPERIMENTAL

A typical synthesis leading to the as-synthesized MCM-48 mesoporous silica was as follows: A 0.745 g (2.05 mmol) of cetyltrimethylammonium bromide (CTAB) was dissolved in 30 g deionized water and then stirred at 30 °C until all CTAB was dissolved. To resulting solution, 15 mL ethanol was added and the mixture was further stirred for 5 min. After the addition of 4 mL ammonia (27 % solution, 56 mmol) and kept for 20 min, 1.2 mL (5 mmol) tetraethylorthosilicate (TEOS) was added and the mixture was stirred under 200-400 rpm for further 10 h. The composition of the initial gel typically was 1.0 TEOS/0.41 CTAB/11.2 NH_3 (27 % solution)/53 EtOH/344 H_2O. The resultant white solid was separated by filtration, washing with distilled water and drying at 70-80 °C overnight. Finally, in order to remove the organic templates, we adopted two different procedures: (i) the elimination of the surfactant by calcination of the above as-synthesized solid at 550 °C for 6 h with a heating rate of 2 °C /min and (ii) the removal of the surfactant from the above as-synthesized solid using the H_2O_2 post-hydrothermal treatment: 0.5 g of the above dried as-synthesized solid was mixed with 60 mL of H_2O_2 (30 % solution) and sealed in an autoclave, followed by heating in an oven at 100 °C for 24 h. The final (porous) material was filtered off, washed with distilled water and ethanol and vacuum dried at 70-80 °C overnight.

Characterization: Powder X-ray diffraction patterns were recorded on a Philips X'Pert PRO SUPER diffractometer operating with nickel-filtered Cu-Kα radiation. Transmission electron micrographs (TEM) were taken on a Jeol-2010 electron microscope operating at 200 kV N_2 adsorption-desorption isotherms were obtained at 77 K on an Omnisorp 100CX instrument. The pore size distributions were determined from the desorption branch of the isotherms with the Barrett-Joyner-Halenda (BJH) method and the specific surface area values were calculated using the BET model. Infrared spectrum was obtained with a Bruker Vector-22 FT-IR spectrophotometer with KBr discs. Thermogravimetric analysis was carried out on a Perkin-Elmer TGA7 themogravimetric analyzer with a heating rate of 10 °C/min under nitrogen atmosphere.

RESULTS AND DISCUSSION

XRD and TEM characterizations: The as-synthesized mesoporous silica and calcined sample exhibit an XRD pattern characteristic of the MCM-48 cubic (space group Ia3d) structure with a high-intensity peak and two additional higher order peaks (Fig. 1, curve a and b), which can be indexed as (211), (220) and (332) diffraction peaks, respectively. The well-resolved peaks indicate that the as-synthesized mesoporous silica possesses the higher order structure. After eliminating surfactant

by calcination or H_2O_2 post-synthesis hydrothermal treatment, only one peak exits at the 2θ of 1-10° range. The main XRD lines are broadened and shifted to higher 2θ values (Fig. 1, curve c), indicating a consequence of the network shrinkage and the order is decreased. Obviously, the lattice distance contraction of calcined sample is larger than that of the H_2O_2 hydrothermal treated. In practice, the surfactant elimination procedure affects the position of the (211) reflection (and consequently the a_0 parameter), which appears shifted to higher 2θ values for calcined sample. Compared to calcined sample, the (220) reflection peak of the H_2O_2 hydrothermal treated is not observed, suggesting the presence of not the ordered MCM-48 cubic structure after the surfactant elimination, as indicating by TEM image (Fig. 2b) which shows a wormlike mesoporous array. The TEM images of the H_2O_2 hydrothermal treated sample indicate the formation of spherical silica nanoparticles with a diameter of 350-400 nm (Fig. 2a).

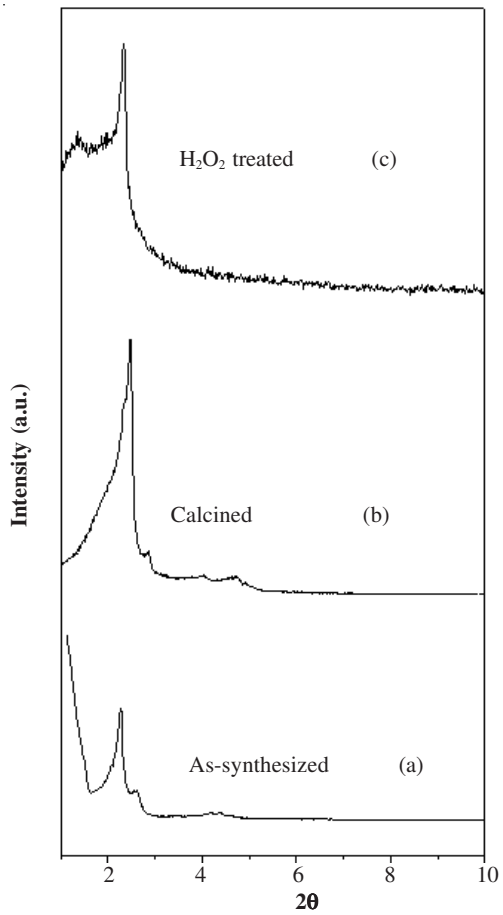

Fig. 1. Powder XRD patterns of (a) as-synthesized, (b) calcined and (c) H_2O_2 hydrothermal treated sample

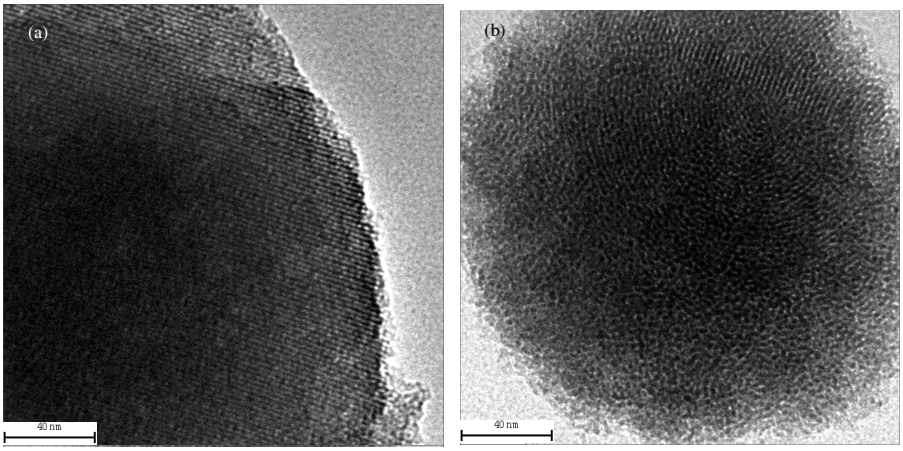

Fig. 2. Representative TEM micrographs of calcined MCM48 (a) and H_2O_2 hydrothermal treated material (b), showing the existence of double-mesopores

Nitrogen adsorption-desorption isotherms: The information derived from the N_2 adsorption-desorption isotherms (Fig. 3) is in agreement with the XRD patterns. The isotherm for the calcined MCM-48 material is a typical reversible type IV adsorption-desorption isotherm (Fig. 3a). The sharpness of the isotherm in range $0.20 < P/P_0 < 0.35$ corresponds to mesopore size. The hysteresis loop in nitrogen adsorption-desorption isotherm at low relative pressure (*ca.* 0.20) reflects its uniform mesopore diameter, which limits the emptying and filling of the accessible volume[17]. The Barrett-Joyner-Halenda (BJH) model analysis of this material provides one quite narrow peak centered at 2.4 nm in the pore diameter distribution (Fig. 3a, the inset), indicating the existence of uniform mesopores. The presence of bimodal pore systems in the H_2O_2 hydrothermal treated material is illustrated by the nitrogen adsorption-desorption isotherm (Fig. 3b). The curve shows two well-defined adsorption steps. The first, at an intermediate relative pressure ($0.20 < P/P_0 < 0.35$), is characteristic of type IV isotherm and can be related to capillary condensation of nitrogen inside the intra-nanoparticle mesopores. Its sharp curvature suggests the existence of uniform and cylindrical small mesopores (*ca.* 2.5 nm). The second step, at a high relative pressure ($P/P_0 > 0.45$), corresponds to the filling of the large mesopores among the primary nanoparticles. An important distinction between the calcined and H_2O_2 hydrothermal treated sample is the presence of the hysteresis loop for H_2O_2 hydrothermal treated sample at higher relative pressures ($P/P_0 > 0.45$) which is a consequence of N_2 filling the textural mesopores. Interestingly, the BJH model analysis of this material provides one narrow peak centered at 2.5 nm in the pore size distribution and another broader peak in the region of 3-5 nm with an evident maximum at 3.6 nm, showing a dual mesoporous distribution. Desorption branch also displays two distinct steps which suggest that two pore systems with different diameters are present to form a three-dimensional pore structure[18]. Confirmation of a double pore system

was clearly supported by the TEM image (Fig. 2b). Many larger 'holes' can be seen in Fig. 2b. These larger holes are disordered and mixed in the smaller mesopores and they can be regarded as the secondary pores in the pore size distribution region of 3-5 nm. These two pore systems are obviously interconnected.

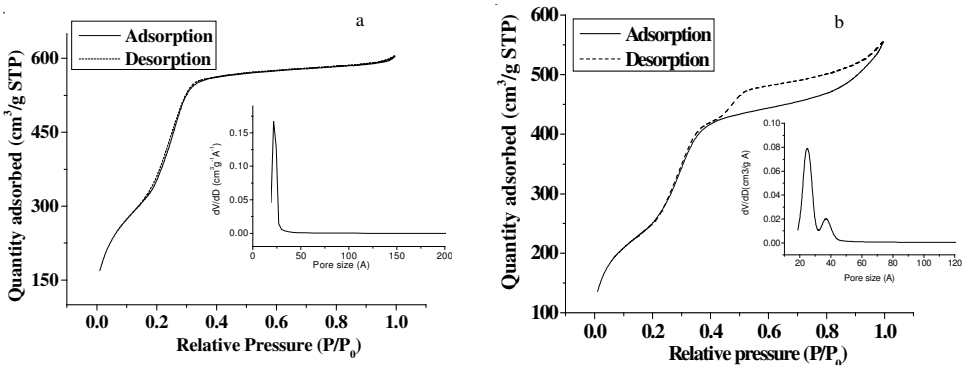

Fig. 3. Nitrogen adsorption-desorption isotherms of (a) calcined and (b) H_2O_2 hydrothermal treated samples and their pore size distribution plots (inserts)

The obvious low surface area and slightly low pore volume of the H_2O_2 hydrothermal treated material (1060 m^2g^{-1}, 0.95 cm^3g^{-1}) when compared to the calcined MCM-48 material (1729 m^2g^{-1}, 1.06 cm^3g^{-1}) can be understood taking into account the thickness of the respective pore walls (estimated from XRD and porosity data). It is noteworthy that the strengthening of the MCM-48 pore wall could favour high thermal and/or hydrothermal stability. On the other hand, the decrease of the surface area and only slight decrease in pore volume indicate the possible interconnection of the pore systems.

FT-IR spectra: IR spectra of all three samples are compared in Fig. 4. The broad band in the range of 3700-3000 cm^{-1} is assigned to a superposition of several stretching modes of Si-OH or H_2O group vibration. The band around 1630 cm^{-1} is attributed to the bending vibrations of water molecules. The bands at 1215, 1090, 800 and 470 cm^{-1} were assigned to symmetric or asymmetric Si-O-Si stretching vibrations. The band at 960 cm^{-1} is generally assigned to Si-O stretching vibration of Si-O-R^+ groups in the as-synthesized state and to Si-OH in the calcined state as well. The band in the range of 3000-2800 cm^{-1} is due to adsorbed substances containing CH groups[19]. Compared to calcined and H_2O_2 hydrothermal treated samples, it can be seen that, after calcination or H_2O_2 hydrothermal treatment, the peaks between 2921 and 2852 cm^{-1} (stretching vibrations of CH_2 and CH_3 groups) almost disappeared. This indicated that after calcination and H_2O_2 hydrothermal treatment, organic moiety was decomposed completely. Interestingly, the H_2O_2 post-hydrothermal treatment can also completely remove organic template, which can be attributed to oxidation decompose of the surfactant molecules under H_2O_2 hydrothermal treatment condition.

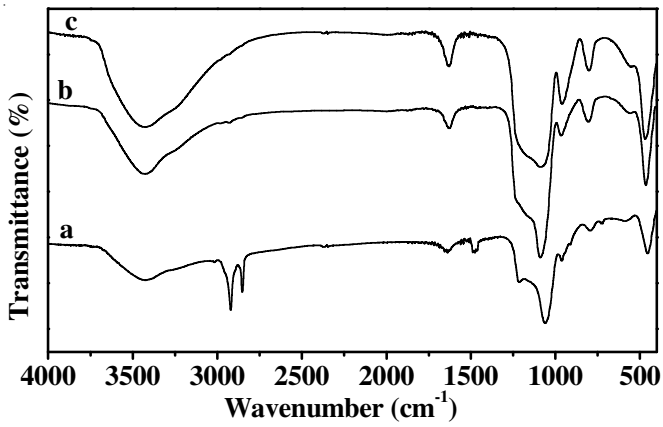

Fig. 4. IR spectra of (a) as-synthesized, (b) H_2O_2 hydrothermal treated and (c) calcined samples

TGA characterization: The TGA patterns compared the weight loss of as synthesized sample and H_2O_2 treated sample heated from room temperature up to 800 ºC at a rate of 10 ºC/min under N_2 atmosphere, as shown in Fig. 5. The TGA patterns have at least three stages of weight loss. As to the as-synthesized sample, a weight loss due to desorption of water amounting to 2.47 % was observed between room temperature and about 100 ºC. The stage of 100-320 ºC corresponding to a weight loss of 49.07 % can be ascribed to the decomposition of the CTAB surfactant species. The weight loss of 7.81 % from 380-800 ºC can be assigned to coke calcination and loss of sianol groups. For H_2O_2 treated sample, the weight loss 2.45 % till 100 ºC and a small weight loss of 2.03 % between 100-320 ºC, from 300-800 ºC, it is 2.18 %, mainly due to the calcination. This indicates that the organic templates were removed completely by H_2O_2 post-hydrothermal treatment.

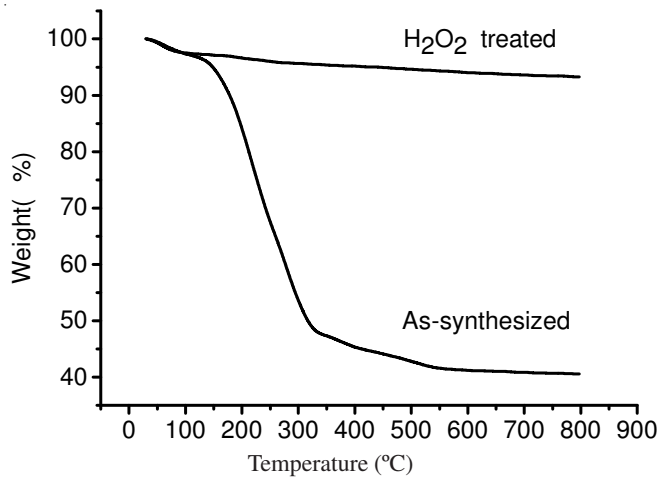

Fig. 5. TGA patterns of as-synthesized sample and H_2O_2 treated sample

Possible formation mechanism of bimodal mesoporous silica: Only after a H_2O_2 hydrothermal treatment did a bimodal mesoporous size distribution arise, it is presumed that H_2O_2 plays an important role. Because H_2O_2 was decomposed to product O_2 and H_2O, O_2 molecules should be penetrate inside the nanochannels more easily than water and such swelled channels leads to the pore size expansion from 2.4 to about 2.5 nm. On the other hand, since the thermal stability of surfactant CTAB is higher (m.p. > 230 °C), the surfactant molecules may be difficult to decompose under 100 °C hydrothermal condition, but it could be decomposed by O_2 oxidation after H_2O_2 hydrothermal treatment, giving rise to some small species which may result in further pore expansion[20] or degradation of part channels. Therefore, the H_2O_2 amount should exceed 60 mL for 0.5 g as-synthesized solid in order to completely remove organic template and simultaneously form ordered bimodal mesoporous silica material. Also, since some surfactant species could be leached out during hydrothermal treatment, the silica walls would tend to collapse inward, making the mesochannels interconnected. However, it should be noted that the creation of the secondary and larger mesopores by the H_2O_2 post-hydrothermal treatment is quite random. It should also be noted that if the H_2O_2 is replaced by ammonia, no similar phenomenon of bimodal mesoporous distribution was observed under the hydrothermal condition. As a result, the oxidation action of H_2O_2 hydrothermal treatment is necessary to prepare mesoporous silicas with bimodal porous systems.

Conclusion

In summary, we report here on a novel preparative procedure yielding narrow distributed bimodal mesoporous silicas by using H_2O_2 post-hydrothermal treatment. The bimodal mesopores are framework pores and mesochannels interconnected. It is believed that H_2O_2 plays an important role in simultaneously removing organic template and forming ordered bimodal mesopores. Taking into account the quick and convenient preparation of the bimodal mesoporous materials under mild hydrothermal condition, it is expected that have a large range of possible applications such as catalysis and sorption.

ACKNOWLEDGEMENT

This work is partly supported by Huainan Science and Technology Agency, P.R. China (Grant No. 2009A05021).

REFERENCES

1. C.T. Kresge, M.E. Leonowicz, W.J. Roth, J.C. Vartuli and J.S. Beck, *Nature*, **359**, 710 (1992).
2. G.P. Yong, Z.X. Jin, H.W. Tong, X.Y. Yan, G.S. Li and S.M. Liu, *Micropor. Mesopor. Mater.*, **91**, 238 (2006).
3. D. Zhao, J. Feng, Q. Huo, N. Melosh, G.H. Fredrickson, B.F. Chmelka and G.D. Stucky, *Science*, **279**, 548 (1998).
4. M. Kruk, M. Jaroniec, C.H. Ko and R. Ryoo, *Chem. Mater.*, **12**, 1961 (2000).
5. J. Yu, J.L. Shi, L.Z. Wang, M.L. Ruan and D.S. Yan, *Mater. Lett.*, **48**, 112 (2001).
6. Y. Yuan, J.L. Blin and B.L. Su, *Chem. Commun.*, 504 (2002).

7. T. Sen, G.J.T. Tiddy, J.L. Casci and M.W. Anderson, *Angew. Chem. Int. Ed. Engl*., **42**, 4649 (2003).
8. D. Kuang, D. Bresensinski and B.J. Smarsly, *J. Am. Chem. Soc*., **126**, 10534 (2004).
9. L. Huerta, C. Guillem, J. Latorre, A. Beltran, R. Martinez-Manez, M.D. Marcos, D. Beltran and P. Amoros, *Solid State Sci*., **8**, 940 (2006).
10. F.Q. Zhang, Y. Yan, Y. Meng, Y.L. Xia, B.Tu and D.Y. Zhao, *Micropor. Mesopor. Mater*., **98**, 6 (2007).
11. X.D. Ma, H.W. Sun and P. Yu, *J. Mater. Sci.*, **43**, 887 (2008).
12. K. Suzuki, K. Ikari and H. Imai, *J. Am. Chem. Soc*., **126**, 462 (2004).
13. M. de Vos and H. Verwij, *Science*, **279**, 1710 (1998).
14. H. Mori, M. Uota, D. Fujikawa, T. Yoshimura, T. Kuwahara, G. Sakai and T. Kijima, *Micropor. Mesopor. Mater*., **91**, 172 (2006).
15. A. Keshavaraja, V. Ramaswamy, H.S. Soni, A.V. Ramaswamy and P. Ratnasamy, *J. Catal*., **157**, 501 (1995).
16. H.P. Lin, C.Y. Mou and S.B. Liu, *Adv. Mater*., **12**, 103 (2000).
17. D.T. On, S.M.J. Zaidi and S. Kaliaguine, *Micropor. Mesopor. Mater*., **22**, 211 (1998).
18. S.A. Bagshaw, *J. Mater. Chem*., **11**, 831 (2001).
19. C.M. Parler, J.A. Ritter and M.D. Amiridis, *J. Non-Cryst. Solids*, **279**, 119 (2001).
20. A. Sayari, P. Liu, M. Kruk and M. Jaroniec, *Chem. Mater*., **9**, 2499 (1997).

(*Received*: 16 September 2009; *Accepted*: 17 February 2010) AJC-8451